- Technical paper -

INFLUENCE OF TOP FLANGE TO SHEAR CAPACITY OF REINFORCED CONCRETE T-BEAMS

Withit PANSUK*[1], Yasuhiko SATO*[2], Ryosuke TAKAHASHI*[3], Tamon UEDA*[2]

ABSTRACT: In this paper, how the top flange area affects shear capacity of RC T-beam with shear reinforcement is discussed based on experimental and analytical observations. The changing in shear crack angle and effect of top flange on concrete strain of T-beam observed in both experimental and analytical results are discussed.
KEYWORDS: T-beams, Top Flange Area, Shear Strength, and 3D Finite Element Method

1. INTRODUCTION

In the slab-beam-girder construction system, the beams are usually built monolithically with the slab. Hence, the portion of concrete slab, effectively connected together with beam, can be considered as the flange projecting from each side of beam. At the same time, the part of beam at the bottom of slab is working as the web of T-shaped beam or simply T-beams.

As well known, in the current design code, shear strength can be calculated based on the modified truss theory, in which effects of top flange area of T-beam cannot be considered. However the area of top flange may affects shear capacity when a beam would fail in shear compression mode. To predict the shear capacity of T-beam more precisely, the effect on shear resisting mechanism must be clarified.

Recently, study on shear resisting mechanism by finite element method has received considerable attention because of its advantages. For example, the well-confirmed finite element program can predict the structural behavior of concrete members with less time and money consumptions than the testing in the laboratory. Of course the most important benefit of this method is enable to get more information such as stresses and strains at any location of members.

In this paper, how the top flange area affects shear behavior of RC T-beam with shear reinforcement is discussed based on experimental and analytical investigations. Shear behavior of rectangular and T-beams, such as load-displacement curve, shear strength, stress development in stirrup are simulated by 3D finite element analysis with the aim of applicability verification of the analysis and finding some information about the shear resisting model of T-beam for the future.

2. EXPERIMENTS

2.1 OUTLINE OF PROGRAM

Two reinforced concrete beams of rectangular and T-shape sections were tested. The rectangular beam had the size of 3800×150×350 mm (length×width×height) and effective depth

*[1] Department of Civil Engineering, Hokkaido University, Graduate student, Member of JCI
*[2] Department of Civil Engineering, Hokkaido University, Dr. E., Member of JCI
*[3] Port and Airport Research Institute, Yokosuka, Research Engineer, Dr. E., Member of JCI

of 300 mm. For T-shaped, the cross section was almost the same as rectangular beam; only concrete flange was attached in the top position of a whole long beam. The stirrups in the tested part had the spacing of 110 mm, while stirrups were placed heavier in the remaining parts of beam to ensure the shear failure within the tested part. The full details of their dimensions, arrangement of reinforcing steel and loading condition are shown in **Fig.1**.

2.2 MATERIALS

Both specimens had the same tension and compression reinforcement, four of D25 and two of D10 respectively. Shear reinforcement was D6 stirrup with closed-hoop shape. **Fig.2** shows cross sections of the specimens. Concrete cylinder strength (f_c') for each specimen was 35 MPa. The main reinforcement ratio (ρ_l) and shear reinforcement ratio (r_w) were 4% and 0.4%, respectively. The properties of steel used are given in **Table 1**.

2.3 TEST METHOD AND MEASUREMENT

Both specimens were tested in a 1000 kN capacity hydraulic testing machine with the simply supported condition over a span of 3000 mm. The load was applied through a steel loading beam with the spherical bearing unit at the both load points. Steel plates 90 mm wide by 15 mm thick were used to distribute loads and support reactions.

For both specimens, the load was applied in 10 kN increments until 180 kN and released until zero. And, the load was applied in the same increments again until failure. After each load increment was stabilized, strains in the tension and web reinforcement, concrete strains in the top part of the beam, and deflections were measured, and crack patterns were noted. Strain gages were attached to measure strain in each stirrup at distances of 60, 130 and 220 mm above the centroid of the tension reinforcement for both specimens. Also, strain gages were attached to measure strains in main bars at distances of 350, 525, 700, 965 and 1500 mm from support for checking yielding of the bars.

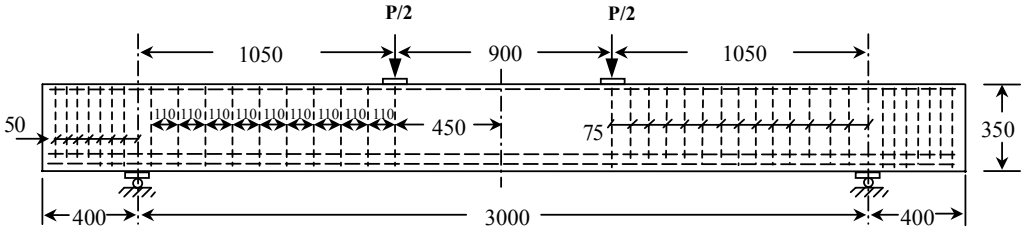

Fig.1 Loading condition and stirrup arrangement (unit: mm)

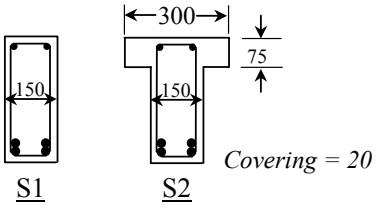

Fig.2 Cross sections (unit: mm)

Table 1 Properties of bars

Bar No.	Area (mm^2)	Yield point (MPa)	Elastic modulus
6	31.67	300	165000
10	71.33	360	192000
25	506.7	400	178000

3. OUTLINE OF FINITE ELEMENT ANALYSIS

3.1 FINITE ELEMENT PROGRAM

In the present study, the 3D nonlinear finite element program developed at the Hybrid Structure Engineering Laboratory of Hokkaido University is used. Three-dimensional 20 nodes iso-parametric solid element, which contains 8 gauss points, can be used for representation of

elements. The smeared crack concept and the fixed crack model are adopted. When taking consideration to the case of three cracks occurs at one gauss point, the application method for each constitutive law is to change the crack from the local coordinate system indicating the principle stress to the plane coordinate system. The constitutive laws used in the program are described below.

Stress of the reinforced concrete elements are expressed by the superposition of the behavior of steel and concrete, at this point, tri-linear model presented by Maekawa et al [1] expressing a reduction of the rate of the strain hardening in the large strain region is adopted.

The 3D Elasto-Plastic Fracture Model [2-4] is adopted for the concrete before a crack. The adopted failure criteria that acted in agreement with Niwa's model in tension-compression zone and Aoyanagi and Yamada's model in tension-tension region are extended to three-dimensional criteria by satisfying boundary conditions [5].

When the first crack occurs, the concrete element under uni-axial stress in the direction perpendicular to crack plane within the local coordinate system is calculated by Reinhardt's tension- softening model [1]. Besides, in other two axes, which intersect perpendicularly which the maximum principle stress, the model proposed by Vecchio&Collins [1] is used for the principle stress-strain relationship. Shear stress acting on the plane intersecting perpendicularly with a crack, is computed by using the average shear stiffness between shear stiffness of crack plane and shear stiffness from the concrete, which does not contain any cracks. Also, a simplified model of shear transfer model developed by Li and Maekawa et al [1] is used in the present finite element program.

At the time of second and third crack, the active crack method [5] that considers the change of concrete element by focusing on the crack width is adopted. However, since this method cannot apply when 2 non-intersecting cracks occur at the same time, the concrete model for the cracks in parallel direction and averaged shear stiffness model must be applied. In terms of averaged shear stiffness model, stress calculated in the sub crack coordinate system is converted to the active crack coordinate system. And, from this shear stress and shear strain in the active crack coordinate system, the stiffness of this region can be obtained. The compression-tension model is the same as already stated above. Moreover, in the case of several sub cracks occur, this method is adopted to only the sub crack that have a largest strain component in the direction intersecting perpendicular to dominant crack after strains within the global coordinate system are converted to each sub crack coordinate system.

3.2 ANALYZED SPECIMEN

Fig.3 shows the finite element meshes of a quarter model for saving calculation time and memory usage in the computation. They are simply supported beams subjected to two-point monotonic loading. In the analysis, the enforced displacements were given at the loading point, which was the node of steel element attached to specimen.

3.3 FAILURE MODE IN ANALYSIS

In the numerical results, softening of concrete in concrete compression zone was observed at peak load. It can be said that the failure mode is shear compression failure. Hence the analytical investigation in this study from the FE analysis should be applied to beams with shear compression failure mode.

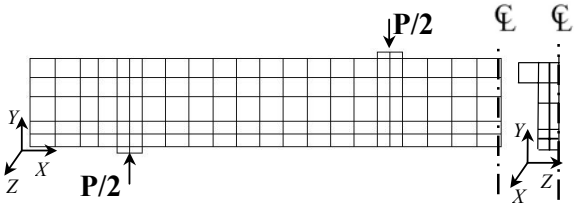

Fig.3 Finite element mesh

4. RESULTS AND DISCUSSION

4.1 LOAD-DEFORMATION CURVES

Fig. 4 shows the experimental and numerical load-deflection curve for specimens S1 and S2. It is very clear from the curve that the load-deformation relationship of RC T-beam is changed because of the existing of concrete top flange. And, the shear strength of T-beam is also higher than that of the rectangular. The FEM results show the same tendency. Moreover, it can be seen that the experimental ultimate load are well predicted. Some examples of well-predicted results using the 3D program are also shown in the previous work [6].

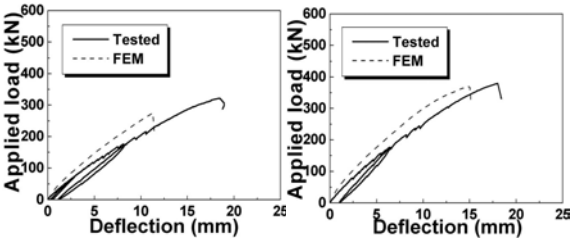

(a) Rec-beam (b) T-beam

Fig.4 Load-deflection curves

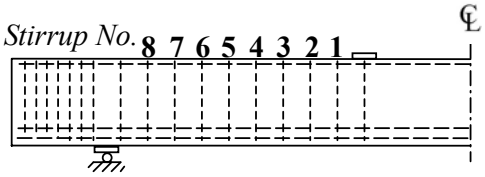

Fig.5 Location and reference number of stirrup whose strains were measured in both specimens

4.2 STRESS IN SHEAR REINFORCEMENT

A typical pattern of the stress variation in stirrups for increasing loads was measured by the strain gages. The stresses plotted are the average for 3 locations of the stirrups in the tested part of the beam. The location and reference number of stirrups whose strains were measured in the experiment are shown in **Fig.5**. From **Figs.5** and **6**, the average stress of selected stirrups in the rectangular and T-beam are compared. It can be seen that the average stress of stirrup for both specimens are almost the same at the initial condition. After that, the average stress of stirrup in the T-beam becomes lower than that in the rectangular beam at around 300 and 250 kN of applied load at stirrup numbers 1,2 and numbers 5,6 respectively. Correspondingly, the load 300 and 250 kN were observed from the experiment that they were the load step that made the crack propagate into the concrete top flange at the same location of the considering stirrups (location near loading point for 300 kN and around mid of shear span for 250 kN, see **Fig.10**). It can be considered that the lower stress of stirrup in the T-beam is due to the increasing of resisting of shear force by concrete in the top flange. This also confirms the importance of top flange in the shear problem. Analyzed and measured stresses in stirrup numbers 5 in the specimen S1 and S2 are shown in **Fig.7**. It is clearly seen that the FEM results can predict the stress development in stirrup well, even if the FEM results have no unloading and reloading part.

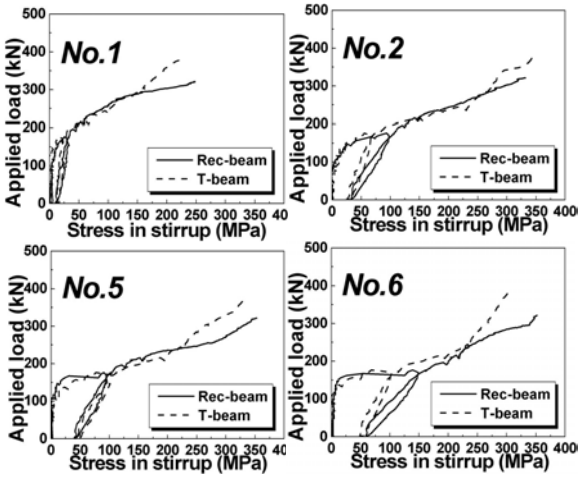

Fig. 6 Comparison of stress in stirrup at different load step

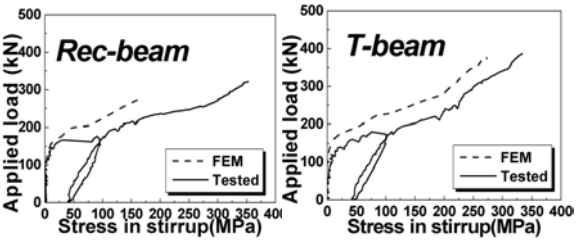

Fig. 7 Comparison of analyzed and measured stress in stirrup

4.3 CRACK PROPAGATION

Crack patterns in the experiment were observed as shown in **Figs.8** and **10**. And, analytical crack pattern are shown in **Figs.9** and **11**. It was observed from the experiment that the crack angle in T-beam is quite large and parallel to each other at the initial shear crack period. However at around ultimate load, the shear cracks with small crack angle occurred. The same result can be simulated by FEM; the cracks with the large crack angle occurred and followed by cracks with smaller crack angle. The "second" cracks in the analytical results are shown in **Fig.11**. This unique was not found in both experimental and analytical results of the rectangular beam (see **Figs.8** and **9**). It can be said that the crack angle is not constant at 45 degrees as in the assumption of the current design code. The real crack angle of T-beam should be used for consideration for the original shear resisting mechanism of T-beam in the future.

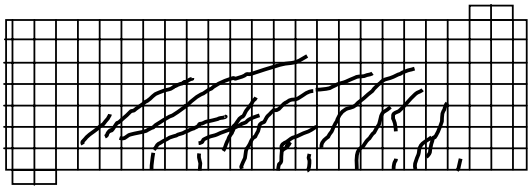

Fig.8 Crack pattern of rectangular Beam at ultimate state

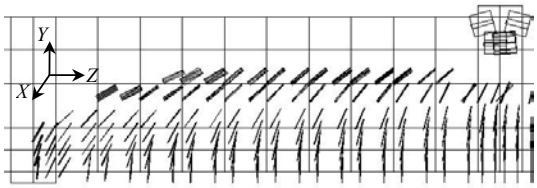

Fig.9 Analytical cracks of rectangular beam at the load step around failure

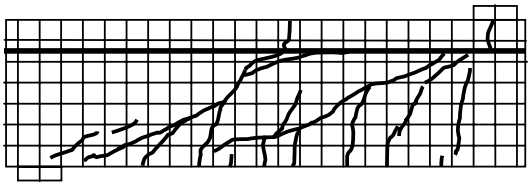

Fig.10 Crack pattern of T-beam at ultimate state

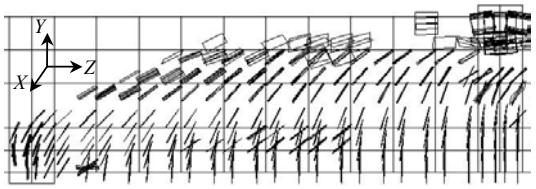

Fig.11 Analytical cracks of T- beam at the load step around failure

4.4 FAILURE MODE

After shear crack occurred, both specimens can sustain the increasing shear force until the failure of concrete in compression zone was obviously observed at ultimate state. Hence, it can be said that both specimens failed in shear compression failure mode. In the case of T-beam, the compression failure in concrete top flange of T-beam was found. In order to compare the failure location with numerical result, the Gauss points from the many locations are selected and the shear stress-strain relationships on the plane *yz* of the global coordinate system are considered. Finally, the strain-softening portion in shear stress-strain curves, which indicates fracture of concrete, is found from the Gauss points in the concrete elements around the loading steel elements as shown in **Figs.9** and **11**.

4.5 CONCRETE STRAIN IN TOP PART OF SPECIMENS

In the experiment, the 2 types of strain gages for concrete, inside concrete and at concrete surface, were installed into both specimens for measuring strain in *X* (parallel to main bars) direction. The measured section is at the concrete compression zone (at the location of stirrup No.1 in **Fig.5**) as shown in **Fig.12**. From the observation, the relation between strains at measured points is constant from the initial condition until the ultimate condition so the only one load level (250 kN) are selected and discussed here. Taking consideration on the comparison of average concrete strain form rectangular and T-beam, it can be seen that the average strain in rectangular beam is higher than the average strain in T-beam for all measured points in *Z* direction, as shown in **Fig.12**. It can be said that the existing of concrete flange can reduce stress resisting by concrete in the web. From **Fig.12**, it also can be seen that the tendency of strain distribution in concrete top

flange is decreasing with the increasing of distance in *Z* direction. In order to compare the measured average concrete strain with numerical result, the concrete strains from Gauss points at around the same location are selected and the average concrete strain and distance along *Z*-axis are considered and shown in **Fig.12**. It was found that the numerical results of both specimens have a good agreement with the experimental results. From this fact, it can be said that the strains are not constant in the flange in *Z* directions. Therefore, the concept of average strain or stress on the appropriate flange area should be considered for the shear resisting mechanism of T-beam in the future work.

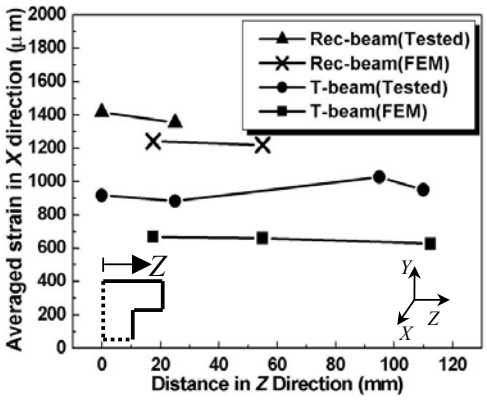

Fig.12 Average concrete strains at section of compression zone

5.CONCLUSIONS

The following conclusions can be drawn from the facts found in this study.

1. Existing of concrete top flange has significant effects on shear behavior of RC T-beams, for example, shear strength, stress in shear reinforcement and crack propagation.
2. Shear behavior, such as load-displacement curve, shear strength, stress development in stirrup and crack propagation, of T-beams can be predicted well by the 3D FE analysis in this study.
3. Changing in crack angle in the case of T-beam is the important data to clarify the shear resisting mechanism of T-beam in the future.
4. Concrete top flange can reduce strain of concrete in the web. For original shear resisting mechanism of T-beam, concrete top flange near compression zone should be considered with average stress on the appropriate flange area.

REFERENCES

1) Takahashi, R., Sato, Y., Ueda, T., "A simulation of shear failure of steel-concrete composite slab by 3D nonlinear FEM," Journal of Structural Engineering, JSCE, Vol.48A, Mar. 2002, pp.1297-1304. (In Japanese)
2) Maekawa, K., Takemura, J., Irawan, P., and Irie, M., "Continuum Fracture in Concrete Nonlinearity Under Triaxial Confinement," Proceedings of JSCE, No.460/V18, Feb. 1993, pp.113-122.
3) Maekawa, K., Takemura, J., Irawan, P., and Irie, M., "Plasticity in Concrete Nonlinearity Under Triaxial Confinement," Proceeding of JSCE, No.460/V18, Feb. 1993, pp.123-130.
4) Maekawa, K., Takemura, J., Irawan, P., and Irie, M., "Triaxial Elasto-Plastic and Fracture Model for Concrete," Proceeding of JSCE, No.460/V18, Feb. 1993, pp.131-138.
5) Okamura, H., Maekawa, K., "Nonlinear Analysis and Constitutive Models of Reinforced Concrete," Gihodo-Shuppan Co. Tokyo, May 1991.
6) Pansuk, W., Sato, Y., Ueda, T., and Takahashi, R., "Investigation on Shear Capacity of Reinforced Concrete T-Beams Using 3D Nonlinear Finite Element Analysis," Journal of Structural Engineering, JSCE, Vol.50A, Mar. 2004, pp.991-998.